

A temperature measurement system with high resolution and low noisess

Bing Zhang^{*}, Xiaoyi Zhu^{*,‡}, Xiaofeng Zhang^{*,§}, Bing Xue^{*}, Hong Liang[†], Jiang Li^{*} and Peng Su^{*}

^{*}*Institute of Earthquake Forecasting,
China Earthquake Administration, Beijing, China*

[†]*Innovation Academy for Microsatellites of the CAS, Shanghai, China*

[‡]*zxy_bj2008@126.com*

[§]*zhangxf@microstate.com*

^{*}*On behalf of The Taiji Scientific Collaboration*

Received 15 September 2020

Revised 16 October 2020

Accepted 30 October 2020

Published 29 March 2021

Due to the temperature fluctuation, both the self-gravity disturbance level of the gravitational wave detection vehicle and the laser interference measurement system are affected, which brings great noise to the gravitational wave measurement, and the temperature field fluctuation has become one of the most important noise sources of the inertial sensor. In order to ensure the noise level of the inertial sensor to meet the needs of detection, this paper uses the AC bridge to reduce the self-noise of the temperature measurement system, improve the resolution of the temperature measurement system, and realize a high-resolution and low-noise temperature measurement system. The experimental results show that the effective value of self-noise of the temperature measurement system is about $3.65 \times 10^{-5}^{\circ}\text{C}$, and the long-period noise is less than $1 \times 10^{-5}^{\circ}\text{C}$. It can be used in the space gravitational wave detection test and control system.

Keywords: Gravitational wave detection; temperature measurement; noise suppression.

PACS numbers : 06.90.+v; 04.30.w; 85.40.Qx

1. Introduction

The space gravitational wave detection vehicle is the payload bearing platform for the scientific detection of space gravitational wave. The gravitational wave detection vehicle produces structural micro-deformation due to temperature fluctuation, material degassing and other reasons, thus affecting the level of self-gravitational disturbance and laser interference measurement system, resulting in gravitational wave measurement noise.

^{*,§}Corresponding authors.

^{*}For more details, please refer to article 2102002 of this Special Issue.

The theoretical analysis and prediction of the detection system point out that the radiometer effect, radiation pressure fluctuation and centroid position fluctuation caused by the temperature field fluctuation near the core inertial sensor test mass will have a great impact on the measurement results, such as the temperature fluctuation of $0.1 \text{ mKHz}^{-1/2}$ at room temperature will affect the 2 kg test quality and cause $10^{-15} \text{ ms}^{-2} \text{ Hz}^{-1/2}$ nonconservative force acceleration disturbance in the 1 MHz band. This effect is close to the basic requirement of gravitational wave detection and has become one of the most important noise sources of inertial sensors.¹

In order to ensure the noise level of the inertial sensor to meet the needs of detection, this paper uses the AC bridge to reduce the self-noise of the temperature measurement system, improve the resolution of the temperature measurement system, and realize a high-resolution and low-noise temperature measurement system.

2. Temperature Measurement System Design

The high-resolution temperature measurement system is mainly composed of STM32, temperature measurement sensor R_T , reference resistance R_{REF} , low noise amplifier A, ADC and DAC. Low noise amplifier A is used to amplify the output voltage of the temperature measurement resistor to fit the input voltage range of the ADC. DAC is used to generate measurement excitation signal.² The STM32 controls the DAC to generate the measurement excitation signal, collects the data of the ADC and outputs it through the UART. The overall structure is shown in Fig. 1.

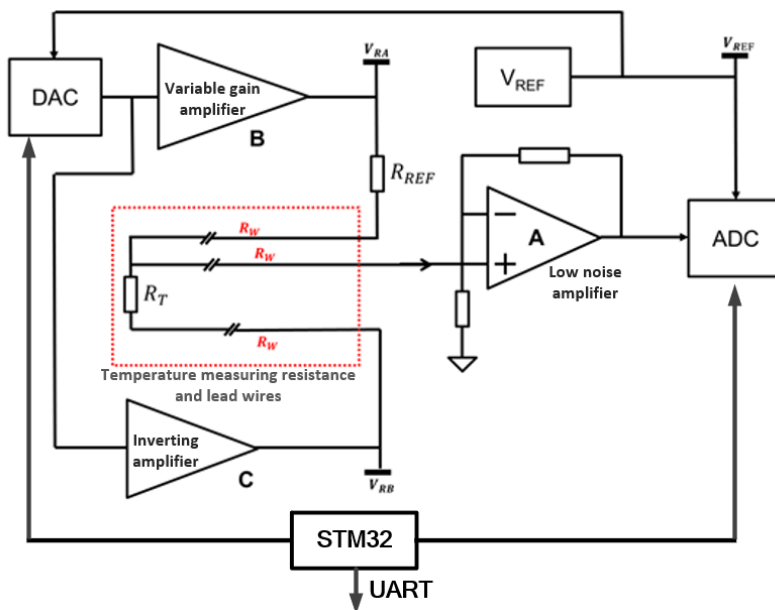


Fig. 1. The overall block diagram.

The DAC output excitation signal is generated by the variable gain amplifier and the inverse amplifier to generate the test excitation signal $V_{RA} = V_R + \Delta V_R$ and $V_{RB} = -V_R$, respectively. The variable gain amplifier is used to set the temperature measurement center point, thus the calculation formula of the measurement temperature is

$$T = \frac{1}{T_C} \cdot \frac{2V_O - \Delta V_R}{V_R + \Delta V_R - V_O} \left(1 + \frac{R_W}{R_{REF}} \right), \quad (1)$$

where V_O is the output voltage of the temperature measuring resistance.

3. Temperature Measurement Sensor Design

The platinum thermal resistance is replaced by the temperature measurement sensor, which advantages contain quite great stable physical and chemical properties, especially the strong oxidation resistance.³ It can maintain ideal characteristics in a wide temperature range (below 1200°C); the resistivity is high and easy to process. It can be made into pretty thin platinum foil or quite fine platinum wire. In the international practical temperature scale IPTS-68, the specified temperature is in the range of -259.34–630.74°C, the platinum thermal resistance is used as the standard instrument to transmit the international temperature scale from 13.81 to 903.89 K. The basic temperature measurement circuit is shown in Fig. 2, and its output voltage is

$$V_O = \frac{R_{REF} - R_T}{R_{REF} + R_T} V_{REF}, \quad (2)$$

where R_T is the temperature measuring resistance. R_{REF} is the reference resistance. V_{REF} is the reference voltage.

For platinum resistive temperature sensor, $R_T = R_0(1 + T_C T)$, if you choose $R_0 = R_{REF}$ resistive temperature sensor, there will be

$$V_O = -\frac{T_C T}{2 + T_C T} V_{REF}, \quad (3)$$

$$\frac{dV_O}{dT} = -\frac{T_C(2 + T_C T) - T_C^2 T}{(2 + T_C T)^2} V_{REF} \approx -\frac{1}{2} T_C V_{REF}. \quad (4)$$

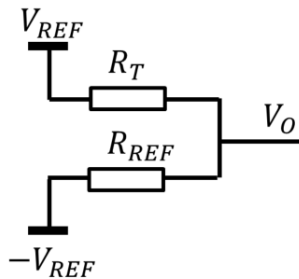


Fig. 2. The basic temperature measurement circuit.

Considering the influence of the thermal effect of the temperature measurement resistance itself, it is necessary to limit the current flowing through the temperature measurement resistor. If the current is I_{REF} , the reference voltage can be taken as: $V_{REF} = I_{REF}R_{REF}$. If Pt1000 is selected as the temperature measurement resistance, $I_{REF} = 0.3 \text{ mA}$, the temperature resolution index of is converted into the voltage resolution index according to formula (2) in order to achieve the temperature resolution of $\frac{10^{-5}\text{K}}{\sqrt{\text{Hz}}}$ @0.0001 Hz~1 Hz

$$\frac{1}{2} \times 0.00385 \times 0.3 \text{ mA} \times 1000\Omega \times \frac{10^{-5}\text{K}}{\sqrt{\text{Hz}}} = \frac{5.775\text{nV}}{\sqrt{\text{Hz}}}$$

The source resistance of the temperature measurement circuit is the parallel value of the temperature measurement resistance and the reference resistance.⁴ The thermal noise is calculated according to 500 Ω . The result is the signal-to-noise ratio of $2.88\frac{\text{nV}}{\sqrt{\text{Hz}}}$, about 6 dB.

Under the condition that the working parameters are constant, using N Pt1000 temperature measurement resistors, the signal-to-noise ratio can be increased by \sqrt{N} times.⁵ For example, if 10 Pt1000 are connected in series as the temperature measurement resistor, the voltage resolution index of the temperature measurement circuit will be changed to $57.75\frac{\text{nV}}{\sqrt{\text{Hz}}}$, source resistance thermal noise to $9.11\frac{\text{nV}}{\sqrt{\text{Hz}}}$, theoretical signal-to-noise ratio of 16 dB, and the total power consumption of the temperature measurement resistance will be about 1 mW. Using 20 Pt1000 in series, the voltage resolution index is $115.5\frac{\text{nV}}{\sqrt{\text{Hz}}}$, theoretical signal-to-noise ratio 19 dB.

In order to achieve the temperature resolution of $\frac{10^{-5}\text{K}}{\sqrt{\text{Hz}}}$ @0.0001 Hz, the time scale reaches 10000 s. Generally, more than five times of continuous recorded data are needed for power spectrum analysis in order to analyze the resolution index of 0.1 mHz–1 Hz band. Because the average temperature change of the test environment is difficult to control within tens of hours, in order to prevent the phenomenon of over-range during data recording, it is appropriate to design a larger full range,⁶ thus chosen to be $\pm 2^\circ\text{C}$.

4. Low-Frequency Noise Suppression Design

The system noise is mainly caused by the conductive characteristics of the components of the electronic circuit and the poor design of the circuit itself, which belong to the internal interference of the system.⁷ The spectrum of system noise is very wide, so the influence of internal noise is mainly considered in the equipment with higher frequency, while in the equipment with lower frequency, the influence of external environment noise and system internal noise should be taken into account.⁸ The noise of the temperature measurement sensor mainly includes shot noise, 1/f noise and resistance thermal noise.

Shot noise is white noise, and its spectrum is flat, that is, the power density is uniform. In addition, shot noise has nothing to do with temperature. In that case, the shot noise is related to the current flowing through the barrier, and the greater the current, the greater the shot noise.⁹ Therefore, under the condition of meeting the temperature measurement resolution, it is necessary to reduce the working current as much as possible

to reduce the shot noise in the system. In the design of the temperature sensor, the maximum working current is 2 mA and the power consumption is 48 mW when the driving voltage is 12 V, so the working current of the temperature sensor is ≤ 2 mA to meet the requirement of reducing shot noise.¹⁰⁻¹³

1/f noise is the real factor limiting the sensitivity of the instrument, especially in the low frequency band, because the output signal of the sensor in the low frequency band, and the semiconductor has a higher noise level in the low frequency band. Moreover, the operational amplifier also has a long period drift, which will also affect the low frequency noise of the system after amplification. The influence of circuit thermal noise on the resolution of temperature measurement is very small and can be ignored.^{14,15}

The range of frequency band in which the resolution of temperature measurement reaches $\frac{10^{-5}K}{\sqrt{Hz}}$, which is the frequency band dominated by 1/f noise. First of all, the influence of the reference source is considered. The V_{REF} in Fig. 2 is the main source of 1/f noise. It can be obtained according to the following formula

$$\frac{dT}{dV_{REF}} \approx \frac{2V_O}{T_C V_{REF}^2} \quad (5)$$

In the case of using twenty Pt1000 in series, $V_{REF} = 6V$, the output voltage corresponding to the full range at 2°C is 0.023 V. According to formula (5), the temperature resolution index $\frac{10^{-5}K}{\sqrt{Hz}}$ can be converted into the noise requirement of V_{REF} , which is $30 \frac{\mu V}{\sqrt{Hz}}$. Considering 1/f noise, it is $300 \frac{nV}{\sqrt{Hz}}$ at 1 Hz frequency point. Therefore, when the output voltage is greater than 6 V, the noise is less than $300 \frac{nV}{\sqrt{Hz}}$ at 1 Hz frequency point, which is the limit condition for selecting the voltage reference source (the reference source of other output voltage can be converted to equal ratio). According to formula (5), the greater the output voltage, the greater the noise influence of the reference source.^{16,17} The 1/f noise of the amplifier and subsequent circuits is suppressed by AC measurement.

5. The Data Processing Design

The DAC output sampling rate is set to 1000 Hz, the sinusoidal signal frequency is 40 Hz, the signal peak value is 12 V and the sampling rate is 500 Hz. The data processing algorithm is realized on STM32, just as follows:

(1) according to the 100 ms time interval, the data of the 200 ms time window is intercepted, and the time window overlaps 100 ms.

(2) the number of intercepted data segments is 100, which is calculated according to the following DFT formula:

$$X(k) = \frac{2}{N} \sum_{n=0}^{N-1} x(n) \left(\cos \frac{2\pi kn}{N} - i \sin \frac{2\pi kn}{N} \right)$$

The module of the calculation result of the above formula is taken as the absolute value of the output result data; if the starting point of the intercepted data is aligned with the zero position of the DAC output sine signal, then the inverse is taken as the symbol of

the calculation result according to the symbol of the imaginary part of the $X(k)$; if it is aligned with the zero position of the DAC output cosine signal, it is taken as the symbol of the calculation result according to the symbol of the real part of the $X(k)$.

(3) the temperature is calculated by using formula (1).

6. Experimental Test and Conclusion

6.1. The test environment

A bucket full of water is used as the test environment, and the temperature sensor is encapsulated in foam. Because the specific heat capacity of the water is large, when the water is placed statically for more than 24 h, the relative temperature change in the water is small and the temperature stabilizes, the temperature resolution test and the system self-noise contrast test are carried out. The test system consists of a reference source, a temperature sensor, a signal amplifier and a 24-bit general data collector, as shown in Fig. 3.

The temperature sensor is placed in a large bucket full of water, the sensor is connected to the temperature measurement circuit, the low distortion signal source DS360 is used as the driving signal, the sensor is driven, and the 24-bit data collector is used to collect the temperature measurement circuit and output the analog signal. As shown in Fig. 4, the collected data are analyzed in two aspects.

6.2. The output test of the temperature measurement system

A sine wave signal with differential 30 Hz, amplitude 10VPP, was output to both ends of the sensor bridge, using DS360. The sensor output signal is amplified by an analog amplifier and input to the first channel of the collector, the signal source output is paralleled to the second channel of the collector, and the acquisition waveform is shown in Fig. 5. The theoretical design of the installation of the collected data is calculated, and the measurement results are obtained as shown in Fig. 6, when the data are processed for one hour, the measured temperature increases from 25.746°C to 25.754°C and changes by

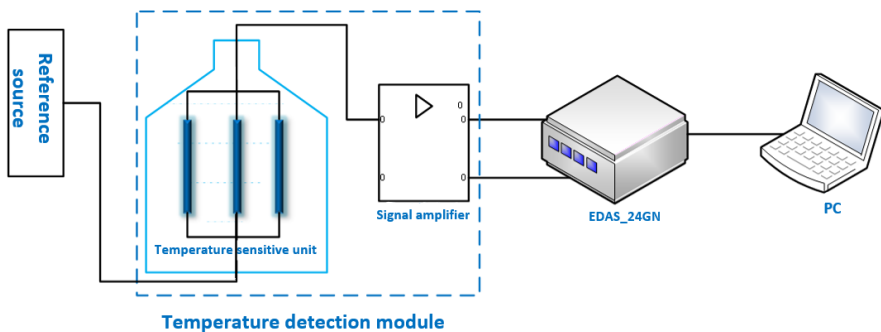


Fig. 3. Experimental system of temperature monitoring.



Fig. 4. Test environment.

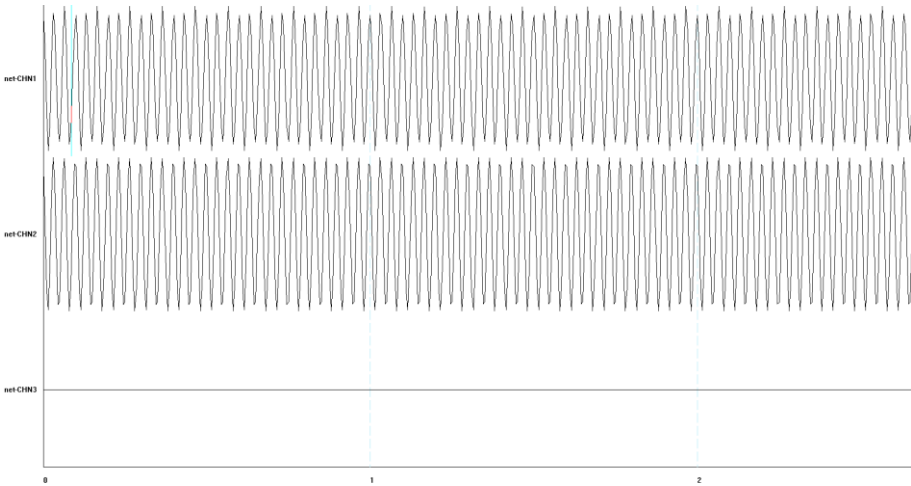


Fig. 5. The respond of 30 Hz excitation signal with an amplitude of 10 V.

0.008°C. The measurement result is always the same as the temperature of the water in the bucket, and the tangent transformation trend is the same, and the whole second calculation method is correct.

6.3. The resolution test of the temperature measurement system

The three sets of sensors all take the waveform of an hour at 4:00 in the morning. The three temperature curves shown in Fig. 7 are the one-hour water temperature curves recorded by three sets of temperature sensors when the driving voltage is 80 V. A total of

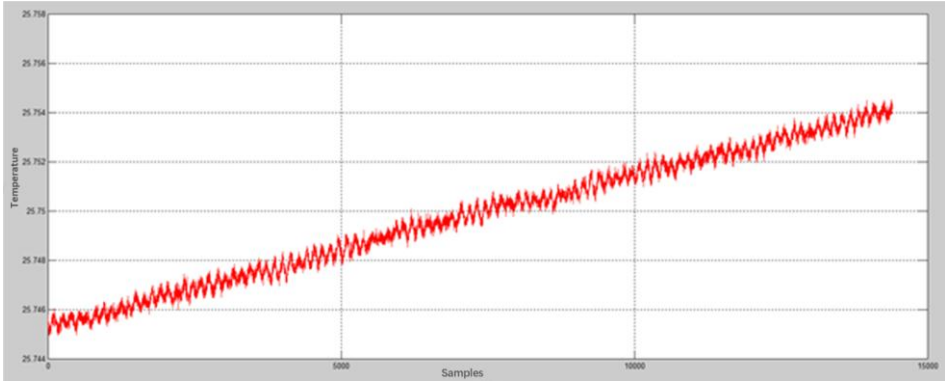


Fig. 6. Temperature measurement results.

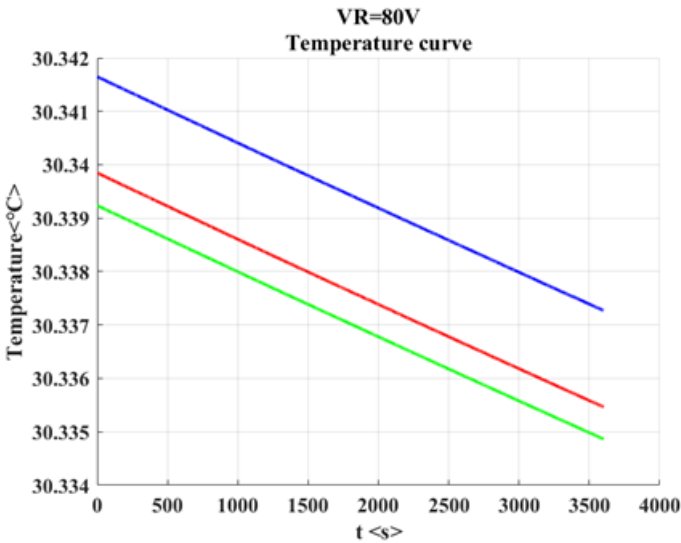


Fig. 7. Water temperature curve.

3600 data points were collected in 1 h. Red represents the amplitude of channel 1, blue represents the amplitude of channel 2, and green represents the amplitude of channel 3. As can be seen from the figure, under the same driving voltage, there is a DC zero deviation (width about 0.02°C) between each channel, the relative waveform amplitude ($24\text{--}30^{\circ}\text{C}$) accounts for less than 0.08%. This shows that the waveform recorded by each channel temperature sensor is very consistent, and there is only a small system deviation.

The power spectrum analysis of the measurement results with three channels is carried out as shown in Fig. 8.

By fitting the self-noise curve, the noise band of $1/f$ is $1/24\text{ h--}0.01\text{ Hz}$ and the noise effective value is $1.92 \times 10^{-6}\text{ }^{\circ}\text{C}$. The band of the white noise is $0.01\text{--}0.5\text{ Hz}$ and the noise

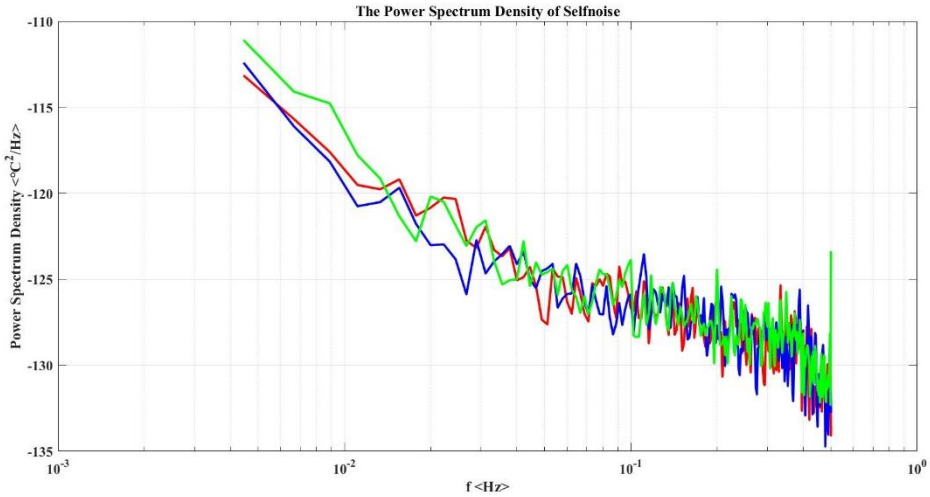


Fig. 8. Power spectrum of temperature measurement system self-noise.

effective value is $4.76 \times 10^{-6} \text{C}$. In the whole frequency band of 0.0001–1Hz, the effective value of self-noise of the temperature measurement system is about $3.65 \times 10^{-5} \text{C}$, which can satisfy the resolution of temperature measurement with long-period noise less than $1 \times 10^{-5} \text{C}$.

Acknowledgments

The authors are very glad to thank the whole Taiji-1 satellite team at Innovation Academy for Microsatellites of the CAS for all their advice and support with this thermal work. This research was supported by the Strategic Priority Program on Space Science, the Chinese Academy of Sciences, Grant No. XDA1502070702, National Key Research and Development Project (2018YFC1503904) and the Special Fund of the Institute of Earthquake Forecasting, China Earthquake Administration (2020IEF0507).

References

1. T. Zhu, S. Huang, L. Shi, W. Huang, M. Liu and K. Chiang, *Chinese Sci. Bull.* **59**, 4631 (2014).
2. Y. Xiaoming, Research on key technology of high resolution temperature sensor for deep well continuous monitoring, Institute of earthquake Prediction, China Seismological Bureau (2018).
3. X.-M. Yang, X.-Y. Zhu and B. Xue, *Earthquake* **38**, 181 (2018).
4. F. S. Feates, D. J. G. Ives and J. H. Pryor, *J. Electrochem. Soc.* **103**, 580 (2019).
5. K. Lee, J. Seong, Y. Han and H. W. H. Lee, *Energies* **13**, 4213 (2020)
6. A. S. Vusikhis, E. N. Selivanov, A. N. Dmitriev, V. P. Chentsov and V. V. Ryabov, *Defect Diffusion Forum* **400**, 4911(2020).
7. F. S. Feates, D. J. G. Ives and J. H. Pryor, *J. Electrochem. Soc.* **103**, 580 (2019).
8. G. F. Zhao, J. Ying, L. Wu and Z. H. Feng, *Sens. Actuator A Phys.* **299**, 111622 (2019).
9. S. Guo, W. Liu, and J. Cheng, *Meas. Sci. Technol.* **30**, 055101 (2019).

10. P. Marjan, *Ponting – Pipenbaher Consulting Eng.* **8**, 214101 (2018).
11. T. G. Gebrie, A. P. Drijarkara and C. S. Kang, *J. Phys. Conf. Series* **1065**, 142022 (2018).
12. V. V. Emets, A. A. Mel'nikov and B. B. Damaskin, *Russian J. Electrochem* **53**, 248 (2017).
13. G. Ferri, F. R. Parente, V. Stornelli, G. Barile and L. Pantoli, *Procedia Eng.* **168**, 1585 (2016).
14. Nanotechnology – Nanowires; Reports Outline Nanowires Findings from Chinese Academy of Sciences (An Integrated Flexible Multifunctional Sensing System for Simultaneous Monitoring of Environment Signals), *Nanotechnology Weekly* (2020).
15. Y. He et al., *J. Neural Eng.* **17**, 045011 (2020).
16. J. Lin et al., *Measurement.* **155**, 107518 (2020).
17. S. Anurag, K. Jyoti and G. Neena, *Mater. Today, Proc.* **28**, 1709 (2020).